Maternal immune activation specifically increases diagonal domain volume in the rat brain during early postnatal development

Tobias C. Wood[1§], Michelle E. Edye[2§], Michael K. Harte[2], Joanna C. Neill[2], Eric P. Prinssen[3] and Anthony C. Vernon*[4, 5]

[1]King's College London, Institute of Psychiatry, Psychology and Neuroscience, Department of Neuroimaging, Centre for Neuroimaging Sciences, De Crespigny Park, London, SE5 8AF, United Kingdom

[2]Division of Pharmacy and Optometry, School of Health Sciences, Faculty of Medicine, Biology and Health, University of Manchester, Manchester, M13 9PT, UK

[3]Roche Innovation Centre Basel, Grenzacherstrasse 124, Basel, CH 4070, Switzerland

[4]King's College London, Institute of Psychiatry, Psychology and Neuroscience, Department of Basic and Clinical Neuroscience, Maurice Wohl Clinical Neuroscience Institute, 5 Cutcombe Road, London, SE5 9RT, United Kingdom

[5]King's College London, MRC Centre for Neurodevelopmental Disorders, New Hunt's House, Guy's Hospital Campus, London SE1 1UL, United Kingdom.

[§]These authors contributed equally to this publication

***Corresponding author:** Anthony C. Vernon (anthony.vernon@kcl.ac.uk); King's College London, Institute of Psychiatry, Psychology and Neuroscience, Department of Basic and Clinical Neuroscience, Maurice Wohl Clinical Neuroscience Institute, 5 Cutcombe Road, London, SE5 9RT, United Kingdom

Running title: Impact of maternal immune activation on rat brain structure in early post-natal life

Keywords: Maternal immune activation; poly (I:C); magnetic resonance imaging; diagonal band; rat.

Abstract: 243 words

Document word count: 4,153

Figures: 2

Tables: 1

Abstract

Maternal immune activation (MIA) is consistently associated with elevated risk for multiple psychiatric and neurological disorders in the affected offspring. Converging lines of evidence from humans and animal models suggest a link between MIA and early entry into an atypical neurodevelopmental trajectory characterised by time- and sex-dependent abnormalities in brain structure and function. However to date, no such studies have investigated the brain-wide impact of MIA in the early post-weaning period, a critical and dynamic window of brain development. To address this, we acquired high-resolution *ex vivo* structural and diffusion tensor imaging (DTI) images from Wistar rat brains on postnatal day (PD) 21 following exposure to the viral mimetic poly (I:C) or sterile saline on gestational day (GD) 15 using a recently validated protocol. Using a combination of atlas-based segmentation and tensor based morphometry analysis we observed that MIA resulted in a significant increase in the relative volume of the diagonal domain (FDR $q<0.1$). Additional trend-level volume increases ($p<0.05$ uncorrected) were also found for the olfactory structures and preoptic area. Although not significant after FDR correction, we found trend-level evidence ($p<0.05$ uncorrected) for MIA x sex interactions in the volume of the diagonal domain, nucleus accumbens, pineal gland and anterior commissure. In contrast to volume, we found no evidence for microstructural alterations in our DTI dataset at PD21. These data provide new insights into the specific effects of MIA early in development, highlighting in particular, the diagonal domain as a target for future studies.

1. Introduction

Epidemiological studies have repeatedly implicated maternal immune activation (MIA) in the aetiology of neuropsychiatric illnesses including schizophrenia and autism spectrum disorder [1, 2]. The development of reverse-translational animal models of MIA based on these human epidemiological findings, whilst restricted in their generalizability to neuropsychiatric disorders *per se*, have documented behavioural, neurochemical, neuroanatomical, and neurophysiological disruptions in the affected offspring [1, 3-5]. These models have thus yielded critical data supporting the predictive potential of epidemiologic studies and uncovered important mechanistic pathways [3]. However, the translatability of these findings to humans remains unclear. One potential approach to circumvent this issue is the coupling of animal models of MIA with non-invasive neuroimaging modalities, including magnetic resonance imaging (MRI) [6]. This approach is advantageous sine MRI permits the non-invasive investigation of large-scale distributed systems and networks across the brain as they develop. In this way, MRI is a powerful, clinically comparable, tool to characterise the brain-wide impact of MIA on brain structure and function. IN turn, it may predicted this would maximise the likelihood of translating findings from animal models to humans and back again to animals [3, 7-12]. Indeed, abnormalities in brain structure and function, as suggested by neuroimaging analyses represent potential endophenotypes for most major psychiatric diagnoses, which may (or may not) be transdiagnostic in nature [13, 14]. Yet only a few studies have attempted to determine whether MIA confers vulnerability to these characteristics. In this context, both ourselves and others have provided evidence for sex-specific deviations from the normal

maturational trajectory of several rodent brain structures that are relevant to psychiatric illness, including the hippocampus, prefrontal cortex and ventricular system [7, 9, 10, 12].

To date however, such studies, including our own, have focussed on the adolescent and adult periods, ignoring prior developmental windows, including the early post-natal period. This is relevant, since this juvenile period is a critical time-window for synaptic circuit formation and maturation, which is both sex-dependent and critical for the proper functioning of brain circuits in adulthood, as required for normal behaviours [15]. To address this gap in our knowledge, using animals prepared at the University of Manchester as part of our joint initiative to establish a robust MIA model in rats, studying early developmental time points (16), we acquired and compared high-resolution, *ex vivo* anatomical MR images and DTI scans from rat offspring (male and female) at PD21 following exposure to MIA or control treatment *in utero* on GD15 [16]. Understanding the impact of MIA on this critical juvenile period at the systems level may provide an important road map, not only to guide future invasive mechanistic studies, but also to serve as a benchmark for longitudinal *in vivo* studies. The overall aim here is to identify novel, non-invasive, cross-species imaging biomarkers that may be predictive of later behavioural dysfunction, against which the efficacy of therapeutic interventions can be tested and evaluated, as suggested by others [17-19]. Our data therefore provide new and important insights into the early effects of MIA on rodent brain development using clinically comparable technology.

2. Methods

2.1 Animals

This *ex vivo* study was performed on a cohort of Wistar rat offspring (male and female), exposed *in utero* either to control (saline) or MIA using polyriboinosinic-polyribocytidilic acid (poly (I:C)). These animals were selected at random from a large cohort of control and MIA-exposed Wistar rats generated at the University of Manchester, which has recently been reported in detail elsewhere [16]. No new animals were therefore generated at King's College London (KCL) for this study and all animal work was undertaken at the University of Manchester. Full details regarding the animals and the induction of MIA are reported in detail elsewhere [16] and in the Supplementary materials and methods herein, in line with recent suggested guidelines for reporting standards for groups using animal MIA models in their research [20]. All procedures adhered to the Animals (Scientific Procedures) Act 1986 and were approved by the University of Manchester AWERB (Animal Welfare and Ethical Review Body).

2.2 Maternal immune activation (MIA)

Induction of MIA in the pregnant dams was performed at the University of Manchester (performed by MEE) and is described in detail elsewhere [16]. Details of the MIA induction may also be found in the Supplementary methods, following recent guidelines [20]. In brief, MIA was induced by a single intraperitoneal injection of poly (I:C) (P9582, potassium salt, Sigma-Aldrich; Gillingham, Dorset, United Kingdom) at a dose of 10 mg/kg on GD 15 in a total of n=32 pregnant Wistar dams, comprising control (saline, CON; n=16)

and MIA (poly (I:C), POL; n=16). At PD21, from this original cohort of n=32 independent litters reported in [16], a control (CON) group, and a MIA group (POL), both comprising n=10 offspring were selected at random. Both experimental groups consisted of male (n=5) and female (n=5) offspring, with no more than n=1 male and n=1 female taken from the same litter. Thus overall, our MRI sample reflects male and female, CON and POL exposed offspring, sampled from 5 independent control litters and 5 independent MIA litters, out of the original cohort of 32 litters (16 control, 16 MIA) generated at the University of Manchester [16].

2.3 Enzyme-linked immunosorbent assay

To confirm successful MIA in the dams, IL-6 concentrations in maternal blood plasma (3 hours post-injection) were determined using a rat-specific ELISA DuoSet (R&D Systems, Abingdon, UK) as reported in [16] as part of a larger study. Briefly, absorbance was measured using a plate reader (MRX, Dynatech, UK) at room temperature, and results were calculated from the standard curve using Prism 6 software (GraphPad, La Jolla, CA, USA). We present here only the IL-6 values (pg/ml) for the specific dams from which offspring were selected for inclusion in the MRI study.

2.4 Tissue preparation for ex vivo MRI

At PD21, the CON (n=10; 5 male, 5 female) and POL (n=10; 5 male, 5 female) offspring randomly selected for MR imaging were culled by cardiac perfusion (0.9% saline followed by 4% paraformaldehyde) under terminal anaesthesia (sodium pentobarbital, 60 mg/kg i.p) and prepared for *ex vivo*

MRI at the University of Manchester as described elsewhere [21]. In brief, fixed brain tissues were kept intact in the cranium and post-fixed for 24 hours in 4% PFA. After which samples were placed in 0.01M phosphate buffer containing 0.05% w/v sodium azide to allow tissue re-hydration prior to MR imaging. Samples were then shipped to KCL and stored at 4°C in this solution for 4 weeks prior to MR imaging. In the absence of pilot data showing the necessary effect sizes, we did not conduct a formal power analysis to establish sample sizes. However, our final group size (n=10) per arm is comparable with both our prior neuroimaging studies in MIA models [7, 10, 12] and those of others [9].

2.5 MR image acquisition

A 7T horizontal small bore magnet (Agilent Technologies Inc. Santa Clara, USA) and a quadrature volume radiofrequency coil (39 mm internal diameter, Rapid Biomedical GmbH) were used for all MRI acquisitions. Fixed brain samples were placed securely one at a time in a custom-made MR-compatible holder and immersed in proton-free susceptibility matching fluid (FluorinertTM FC-70; Sigma-Aldrich). Samples were scanned in a random order, with the KCL operator (ACV) blinded to treatment group (CON or POL) by numerical coding of samples undertaken at the University of Manchester (MEE). Scanning of samples was interspersed with phantoms to ensure consistent operation of the scanner. Two sets of MR images were acquired: a 3D Fast-Spin Echo (FSE) for structural analysis and a DTI protocol for microstructural analysis. The T2-weighted 3D FSE image had the following parameters: TE/TR=60/2000, echo train length = 8, matrix size =

192x128x192 and field of view (FOV) = 28.8x19.2x28.8 mm, yielding isotropic voxels of 150 µm. Total scan-time was 1hr 44min. The DTI scans were acquired using a four shot Echo Planar Imaging (EPI) sequence with TE/TR=35/4000ms, matrix size = 128x96 and FOV = 25.6x19.2mm, with an in-plane resolution of 200µm across 50, 0.5mm thick slices. A total of 30 non-collinear diffusion directions were acquired, with four b=0 images with a target b value of 2000 s/mm. Total scan time was 1hr 22min. Reversed phase-encoded direction DTI images were additionally acquired to correct for eddy current distortions (8min). Total scan duration for the entire protocol was 3hr 14min per brain.

2.6 MR image processing

The raw MR images were downloaded from the scanner server and converted to the NIFTI image file format, inspected for artefacts and then pre-processed as described previously [22]. After elimination of scans with artefacts the final n values per group for statistical comparisons were: Volume; CON, n=9 (4 male, 5 female) vs. POL, n=10 (5 male, 5 female); DTI: CON, n=10 (4 male, 4 female) vs. POL, n=10 (5 male, 5 female). The DTI parameter maps were then calculated, consisting of Fractional Anisotropy (FA) and Medial Diffusivity (MD) as described elsewhere [22]. The FSE structural scan was bias-field corrected and a template image constructed using the 3D FSE MR images from all available subjects in the study (n=19). The resulting 3D FSE template was then non-linearly registered to an open access, high resolution, isotropic, *ex vivo* T2-weighted MRI and DTI atlas of the PD18 Wistar rat brain, referred to hereafter as standard space [23]. MR images from individual offspring were

non-linearly registered to the study template using their T2-weighted FSE images. Logarithmic Jacobian determinants (*J*) were calculated from the inverse warp fields in standard space to estimate apparent volume change [22]. The transforms from native to study template and from study to standard space were concatenated and applied to DTI parameter maps (FA, MD) to align them with the template [22].

2.7 Statistical analysis

A subset of maternal plasma levels of IL-6, consisting of those values only from dams whose offspring were selected for MR imaging (CON vs. POL) were compared using unpaired t-test (2-tailed), with α=0.05, using Prism software (v6.0; GraphPad Inc. La Jolla, CA, USA). For the MR image analysis, group-level differences (contrast = CON vs. POL) in volume (mm^3), FA (unitless) and MD (mm^2 s^{-1}) were assessed using a combination of atlas-based segmentation (ABS) and voxel-wise tensor-based morphometry (TBM) analyses [7]. The Wistar PD18 MRI atlas is parcellated into 26 regions of interest (ROI), as described elsewhere [23]. Using this atlas, we extracted values for volume, FA and MD for all 26 ROIs and calculated total brain volume by the summation of each individual atlas ROI volumes. The volumes for each individual atlas ROI were adjusted for inter-animal variation in total brain volume by expressing these as a percentage of total brain volume [7]. Group-level differences between CON and POL-exposed animals in either volume, FA or MD were assessed for all 26 ROI using 2-way ANOVA with MIA (CON or POL) and sex (male or female) as between and within group factor respectively, using Prism software (v6.0; GraphPad Inc. La Jolla, CA,

USA) with α=0.05. These uncorrected *p*-values from the F-test contrasts (main effects of prenatal treatment, sex and prenatal treatment x sex interaction) were then corrected for multiple comparisons (to account for Type I errors across the 26 ROI) using the False Discovery Rate (FDR) procedure, with the threshold set at 10% (q<0.1) based on prior *in silico* modelling of the sensitivity of rodent brain MR image registration [24]. To complement and extend the atlas based segmentation approach, we also carried out a voxel-wise analysis of apparent volume change from the log-scaled Jacobian determinant maps (Tensor Based Morphometry, TBM), using permutation tests and Threshold-Free Cluster Enhancement (TFCE) in FSL *randomize* corrected for multiple comparisons using FDR as described elsewhere [7]. Sex was included as a regressor of no interest in the design matrix for voxel-wise analysis of the Jacobian determinants and the DTI parameter maps.

3. Results

3.1 Maternal circulating IL-6 levels

An ELISA-based assay revealed a statistically significant increase in circulating levels of IL-6 in maternal plasma samples 3 hours post-injection in POL-injected dams as compared to controls (t=3.62, df=14; *p*=0.007; Cohen's *d* = 2.3; **Supplementary Figure 1**), suggestive of successful induction of a maternal immune response following POL-injection as reported elsewhere for this cohort [16]. A notable variability was present however, in the plasma IL-6

levels within the POL-injected dams (range 480 to 2890 pg/ml; **Supplementary Figure 1**).

3.2 Atlas based segmentation analysis of volumetric and DTI datasets

3.2.1 Juvenile rat brain volume

Whole brain volumes were significantly affected as a function of sex ($F(1,15)=5.89$ $p=0.03$). There were no significant effects of either MIA, or MIA x sex interaction (**Supplementary Figure 2a**). Hence in all animals, the brain region volumes were normalised to the individual's total brain volume. 2-way ANOVA analysis of all 26 ROI revealed main effects of sex on the relative volumes of 3/26 (12%) atlas ROIs, including the bed nucleus of the stria terminalis (BNST), the cerebellum and the ventricular system (pANOVA uncorrected <0.05; **Table 1**). The relative volumes of the BNST and cerebellum appeared smaller in female juvenile rats as compared to males, whereas, in contrast, the ventricular volumes were apparently larger in female juvenile rats as compared to males (**Supplementary Figure 2b-d**). None of these results remained significant after multiple comparisons correction (all q>0.1; **Table 1**). Therefore, they should only be considered trend-level effects.

There were main effects of MIA on the relative volumes of 3/26 (12%) atlas ROIs including the diagonal domain, olfactory structures and preoptic area (pANOVA uncorrected <0.05; **Table 1**; **Figure 1a-c**). For each of these ROI, the relative volumes were apparently increased in POL as compared to CON offspring. However, only the main effect of MIA on the relative volumes of the diagonal domain remained significant after multiple comparisons correction

(q<0.1; **Table 1**; **Figure 1a**). In contrast, the other results did not and may thus only be considered trend-level effects (q>0.1 **Table 1**; **Figure 1b, c**).

Interactions between sex and MIA were found for the relative volumes of a further 4/26 (15%) of the atlas ROIs, including the diagonal domain (**Table 1; Figure 1a)**, nucleus accumbens, pineal gland and anterior commissure (pANOVA uncorrected <0.05; **Table 1; supplementary Figure 3a-c**). However, none of these results remained statistically significant after multiple comparisons correction (all q>0.1; **Table 1**) and again, may only be considered as trend-level effects. Exploratory Bonferroni *post-hoc* testing on these interactions suggests that the apparent volume increases seen in the relative volumes of each structure, including the DD is potentially influenced by sex, (**Figure 1a** and **Supplementary Figure 3a-c**). However, this remains to be confirmed in future studies with a larger sample size.

3.2.1 Juvenile rat brain microstructure (FA, MD)

There were no main effects of sex, MIA or MIA x sex interaction on FA or MD, for any of the ROIs in the Wister PD18 MRI atlas, even at (uncorrected) p<0.05 (*data not shown*).

3.3 Tensor based morphometry and voxel-wise analysis of DTI parameters

TBM analysis revealed no significant differences after correction for multiple comparisons (10% FDR; q<0.1) in relative volumes (indexed as the log scaled jacobian determinant) between CON and POL offspring (**Figure 2**). At an exploratory p-value of <0.01 uncorrected (solid contours; **Figure 2**) there were

bilateral clusters of voxels within the region of the diagonal domain indicating apparent increased volume in POL offspring (male and female) relative to controls, consistent with the atlas-based analysis. At a highly exploratory p-value of <0.05 uncorrected, there were additional sparse clusters of increased volume in POL offspring relative to controls in the nucleus accumbens, septal region and dorsal striatum (dashed contours; **Figure 2**). Consistent with the atlas-based analysis, voxel-wise analysis of FA and MD maps revealed no significant differences between CON and POL offspring either after correction for multiple comparisons (10% FDR) or even at p<0.05 uncorrected (*data not shown*).

4. Discussion

The principle finding of the current study is that prenatal exposure to MIA using poly (I:C) (POL) results in a significantly increased volume of the diagonal domain (DD) in juvenile (PD21) Wistar rat brains. Our data suggest this effect may potentially be sex-dependent (greater in females), although this did not survive FDR correction. In addition, the volumes of the olfactory structures and preoptic area (POA) were also increased in the PD21 rat brain following MIA exposure, albeit only at trend-level significance (p<0.05 uncorrected). We therefore do not discuss these findings further herein, but suggest these may represent important structures to focus on for future studies with larger sample sizes. Our data also suggest that microstructural alterations reported in the adult rodent brains following prenatal MIA exposure [10, 25] may not be present in juvenile offspring, at least at PD21. It would be important however, to check for the presence of finer-scale wiring alterations

that may be undetectable by MRI, for example using monosynaptic retrograde tracing with rabies virus [26].

These new data extend prior work mapping the impact of MIA on the rodent brain. Specifically, we provide here the earliest assessment to date of rat brain volume and microstructure post-MIA, in a critical rodent brain developmental window (PD21), using brain-wide operator-independent analysis methods combined with a carefully validated rat MIA model [16]. We found no significant effects of prenatal POL exposure on the volume or microstructure of the rat hippocampus, prefrontal cortex, corpus striatum or lateral ventricles at PD21. These data suggest that MRI-detectable structural changes in these regions that are of particular relevance to psychiatric illness may only emerge with increasing post-natal age, consistent with prior MRI findings in MIA-exposed rodents from PD35 onwards [7, 9]. These data are also consistent with the suggested age-of-onset of hippocampus volume deficits reported in youth on the psychosis spectrum [27] and in childhood onset schizophrenia [28].

The main novel finding from our study is that the primary region of the juvenile rat brain affected by prenatal POL exposure is the diagonal domain (DD; also referred to as the diagonal band of broca). This is consistent with and extends our observations of volume increases in this region in MIA-exposed rats from PD50 onwards; encouragingly, this is despite methodological differences in the induction of MIA to that in the current work [7, 16]. The DD is part of the basal forebrain, containing cholinergic, glutamatergic and GABA neurons [29,

30]. These send efferent projections to several brain regions, in particular to the hippocampus via the medial septum [29, 30]. During normal rodent brain development, from the third post-natal week (equivalent to our MR imaging window) cholinergic neurons in the DD undergo progressive hypertrophy of the soma and proximal dendrites, followed by shrinkage lasting up to the fifth postnatal week [31]. A single prior study in a mouse poly (I:C) MIA model reported an increase in both the number of cholinergic neurons and the activity of choline acetyltransferase (ChAT), the enzyme responsible for the synthesis of acetylcholine in the DD of MIA-exposed offspring at both E16.5 and PD1, although later time-points were not assessed [32]. However, there is evidence from human *post-mortem* studies for elevated ChAT activity and an increased number of cholinergic neurons in the basal forebrain of autistic individuals, but only in those aged <13 years old [32, 33]. In contrast, no differences in DD volume were found in a *post-mortem* study of individuals with a diagnosis of schizophrenia or an affective disorder compared to controls (mean ages 54±9; 49±12 and 55±10 years, respectively) [34]. We tentatively suggest, based on these data, that our finding of increased DD volume reflects an increase in the number of cholinergic cells and/or hypertrophy of their proximal dendrites [31]. This may only be transiently present following MIA exposure and may normalise with increasing age, as previously seen for other rodent structural brain changes at PD150 following MIA exposure in our prior work [7]. Changes in GABA or glutamatergic neurons and the potential involvement of non-neuronal cell types, including microglia [16, 35, 36] however, remain to be established in follow-up *post-mortem* work.

Irrespective of the cellular basis of increased DD volume, our aforementioned observations coupled with those of others strongly suggest that MIA exposure specifically affects the DD early in rodent brain development. This has potential functional implications that are relevant for the development of psychiatric illness associated with exposure to MIA *in utero*. Specifically, as already stated, neurons in the DD send projections to the hippocampus via the medial septum, which play a key role in the modulation of theta (θ) rhythms in this region [29]. Oscillations in this frequency band are critically important for attention, spatial and working memory [37] and sensory information processing [29]. Of note, decreased θ rhythms are reported in the adult rat hippocampus following exposure to MIA at GD15 [38, 39]. Furthermore, this was accompanied by decreased θ band coherence between the hippocampus and prefrontal cortex, which correlated positively with behavioural impairments in sensory processing [38]. Speculatively, early abnormal development of the DD-medial septum-hippocampus circuit following MIA exposure may be relevant for the development of abnormal hippocampus θ-oscillations, leading to domain-specific behavioural abnormalities in adult offspring, which have relevance for human psychiatric illness.

Limitations of our study should be noted. First, increased power is required to confirm the trend-level results we observed, especially taking into account the evidence that sex influences brain structural differences in MIA models [9]. Indeed, despite detecting significant volume changes in the DD as determined

using atlas based segmentation analysis, our TBM findings of apparent increases in DD volume were only significant at trend-level ($p<0.05$ uncorrected). This is likely due to the greater statistical penalty in terms of FDR correction for voxel-wise analysis as compared to ROI measures. Prior *in silico* work assessing registration sensitivity in rodent MRI datasets suggests that recovering subtle volumetric changes of 5% or less, in small brain structures, is difficult and unlikely to survive conservative multiple comparisons correction [40]. In the case of the DD, the magnitude of the apparent volume increase in the POL-exposed offspring falls inside this range (+4.3%). Hence, it is not surprising this does not survive FDR correction using TBM. Furthermore, our sample size is comparable with both our own prior neuroimaging studies in MIA models [7, 10, 12] and those of others [9]. Second, a longitudinal MR imaging design would have been preferable to increase statistical power, as in our prior work [7] and that of others [9] to map the trajectories of affected brain regions from PD21 onward. Nonetheless, the *ex vivo* data generated in the current study provides the necessary support for such longitudinal studies. Indeed, our data suggest that structural alterations in the DD can be detected at PD21 using *ex vivo* structural MRI at a resolution that is certainly achievable *in vivo*. Knowledge of effect sizes from the current study also allows a more precise calculation of the necessary sample size for future *in vivo* work. For example, using the effect size for the DD volume increase (Cohen's d =1.43) suggests that a minimum of n=14 offspring should be included in each group to achieve α=0.05 with 95% power (G*Power v3.1.9.2). Future longitudinal studies should also seek to combine structural and functional MRI measures to establish the relationship of the MRI findings,

particularly connectivity within in the DD-medial septum-hippocampus circuit, to domain-specific behavioural deficits in this model, such as working or spatial memory. This is critical to establish whether our current MRI findings at PD21 truly reflect pathological changes indicative of early disruption to key brain circuits following MIA. Third, the PD18 rat atlas used in the current study did not include an ROI for the amygdala; hence we could not extract MRI measures for this region for comparison, or to explore any relationship with our measures of circulating maternal IL-6 in the dam. This is relevant since recent human MRI studies suggest a weak, but statistically significant association between maternal circulating IL-6 levels and increased neonatal amygdala volume and functional connectivity, which are in turn, predictive of impulsivity and working memory deficits in the offspring at 2-years of age [8, 41]. However, our TBM analysis found no clusters of voxels in the region of the amygdala with increased apparent volume, even at highly exploratory statistical thresholds. Further studies, potentially including MR imaging of neonatal offspring following exposure to MIA, along with specific manipulation of IL-6 levels in the dam are required to confirm if the human observations regarding MIA and amygdala volume may be successfully back translated.

5. Conclusion

The findings of the current study provide new insights into the early effects of MIA on rodent brain development using clinically comparable technology. They lend further support to the suggestion that prenatal exposure to MIA leads to structural brain changes, in key brain regions that precede later behavioural dysfunction. Specifically, our data suggest the DD and connected

structures as novel targets for future work, including establishment of cellular mechanisms and longitudinal studies to establish the relevance to behavioural phenotypes in this model.

Funding sources: ACV acknowledges financial support for this work from Roche and the Medical Research Council (New Investigator Research Grant [NIRG], MR/N025377/1). The work [at King's College, London] was also supported by the Medical Research Council (MRC) Centre grant (MR/N026063/1). The work [at the University of Manchester] was supported by Roche and the University of Manchester MRC Confidence in Concept Scheme. The funders had no role in the decision to publish this work.

Acknowledgements: The authors thank the British Heart Foundation for supporting the 7T MRI scanner at the King's College Preclinical Imaging Unit (KCLPIU).

Supplementary data: Supplementary data associated with this article can be found in the online version.

Figure and table legends

Figure 1. Region-specific changes in apparent volume of the juvenile (PD21) Wistar rat brain following prenatal exposure to poly (I:C) (POL) or control (CON, saline) at gestational day (GD) 15 as revealed by atlas-based segmentation. (a) Diagonal domain volume; (b) olfactory structures and (c) preoptic area volumes were all increased. Data shown are relative volumes, expressed as a percentage of total brain volume. ★$p<0.05$ main effect of MIA, corrected for multiple comparisons at $q<0.1$ using FDR procedure; *$p<0.05$ main effect of MIA at trend-level significance ($p<0.05$ uncorrected); Δ$p<0.05$, MIA x sex interaction at trend level significance ($p<0.05$ uncorrected).

Figure 2. Voxel-wise tensor based morphometry (TBM) with sex as regressor of no interest also suggests an apparent volumetric increase in the diagonal domain and septal nuclei of the Wistar rat brain at PD21 following *in utero* exposure to poly I:C (POL), relative to sterile saline controls (CON) on GD15. Data shown are the log scaled Jacobian determinant, a simple and direct means of determining local voxel-wise expansion (yellow/red) or compression ((blue / cyan) relative to the reference space (range -10 to +10% change). For transparency, all raw data is shown. Contours are used to represent clusters of voxels with statistical significance ranging from $p<0.05$ uncorrected (dashed lines) to $p<0.0005$ uncorrected (solid lines). No clusters of voxels survived FDR correction at either $q<0.05$ (5%) or $q<0.1$ (10%). Note additional clusters of voxels with apparent volume increases at trend-level significance ($p<0.05$ uncorrected) in the septal nuclei, striatum, and nucleus accumbens and ventral orbital cortex.

Table 1. 2x2 ANOVA statistics for the atlas based segmentation analysis. Only ROIs with significant results (prior to multiple comparison correction) are shown. p-values shown are those from the main effects of either MIA or sex and MIA x sex interaction. q-values indicate significance after FDR correction using the Benjamini-Hochberg procedure at 10% cut-off ($q<0.1$). Post-hoc tests represent exploratory Bonferroni post-hoc tests conducted for any ROI with trend-level evidence for an MIA x sex interaction.

References

[1] S.D. Bilbo, C.L. Block, J.L. Bolton, R. Hanamsagar, P.K. Tran, Beyond infection - Maternal immune activation by environmental factors, microglial development, and relevance for autism spectrum disorders, Exp Neurol, 299 (2018) 241-251.

[2] I. Knuesel, L. Chicha, M. Britschgi, S.A. Schobel, M. Bodmer, J.A. Hellings, S. Toovey, E.P. Prinssen, Maternal immune activation and abnormal brain development across CNS disorders, Nat Rev Neurol, 10 (2014) 643-660.

[3] A.S. Brown, U. Meyer, Maternal Immune Activation and Neuropsychiatric Illness: A Translational Research Perspective, Am J Psychiatry, DOI 10.1176/appi.ajp.2018.17121311(2018) appiajp201817121311.

[4] U. Meyer, Prenatal Poly(I:C) Exposure and Other Developmental Immune Activation Models in Rodent Systems, Biol Psychiat, 75 (2014) 307-315.

[5] U. Meyer, J. Feldon, S.H. Fatemi, In-vivo rodent models for the experimental investigation of prenatal immune activation effects in neurodevelopmental brain disorders, Neurosci Biobehav R, 33 (2009) 1061-1079.

[6] C.J. Finlay, S. Duty, A.C. Vernon, Brain morphometry and the neurobiology of levodopa-induced dyskinesias: current knowledge and future potential for translational pre-clinical neuroimaging studies, Front Neurol, 5 (2014) 95.

[7] W.R. Crum, S.J. Sawiak, W. Chege, J.D. Cooper, S.C.R. Williams, A.C. Vernon, Evolution of structural abnormalities in the rat brain following in utero exposure to maternal immune activation: A longitudinal in vivo MRI study, Brain Behav Immun, 63 (2017) 50-59.

[8] A.M. Graham, J.M. Rasmussen, M.D. Rudolph, C.M. Heim, J.H. Gilmore, M. Styner, S.G. Potkin, S. Entringer, P.D. Wadhwa, D.A. Fair, C. Buss, Maternal Systemic Interleukin-6 During Pregnancy Is Associated With Newborn Amygdala Phenotypes and Subsequent Behavior at 2 Years of Age, Biol Psychiatry, 83 (2018) 109-119.

[9] Y. Piontkewitz, M. Arad, I. Weiner, Abnormal trajectories of neurodevelopment and behavior following in utero insult in the rat, Biol Psychiatry, 70 (2011) 842-851.
[10] J. Richetto, R. Chesters, A. Cattaneo, M.A. Labouesse, A.M.C. Gutierrez, T.C. Wood, A. Luoni, U. Meyer, A. Vernon, M.A. Riva, Genome-Wide Transcriptional Profiling and Structural Magnetic Resonance Imaging in the Maternal Immune Activation Model of Neurodevelopmental Disorders, Cereb Cortex, 27 (2017) 3397-3413.
[11] M.D. Rudolph, A.M. Graham, E. Feczko, O. Miranda-Dominguez, J.M. Rasmussen, R. Nardos, S. Entringer, P.D. Wadhwa, C. Buss, D.A. Fair, Maternal IL-6 during pregnancy can be estimated from newborn brain connectivity and predicts future working memory in offspring, Nat Neurosci, 21 (2018) 765-772.
[12] A.C. Vernon, P.W. So, D.J. Lythgoe, W. Chege, J.D. Cooper, S.C. Williams, S. Kapur, Longitudinal in vivo maturational changes of metabolites in the prefrontal cortex of rats exposed to polyinosinic-polycytidylic acid in utero, Eur Neuropsychopharmacol, 25 (2015) 2210-2220.
[13] Q. Gong, C. Scarpazza, J. Dai, M. He, X. Xu, Y. Shi, B. Zhou, S. Vieira, E. McCrory, Y. Ai, C. Yang, F. Zhang, S. Lui, A. Mechelli, A transdiagnostic neuroanatomical signature of psychiatric illness, Neuropsychopharmacology, DOI 10.1038/s41386-018-0175-9(2018).
[14] L. Schilbach, F. Hoffstaedter, V. Muller, E.C. Cieslik, R. Goya-Maldonado, S. Trost, C. Sorg, V. Riedl, R. Jardri, I. Sommer, L. Kogler, B. Derntl, O. Gruber, S.B. Eickhoff, Transdiagnostic commonalities and differences in resting state functional connectivity of the default mode network in schizophrenia and major depression, Neuroimage Clin, 10 (2016) 326-335.
[15] O. Marin, Developmental timing and critical windows for the treatment of psychiatric disorders, Nat Med, 22 (2016) 1229-1238.
[16] K.N. Murray, M.E. Edye, M. Manca, A.C. Vernon, J.M. Oladipo, V. Fasolino, M.K. Harte, V. Mason, B. Grayson, P.C. McHugh, I. Knuesel, E.P. Prinssen, R. Hager, J.C. Neill, Evolution of a maternal immune activation (mIA) model in rats: early developmental effects, Brain Behav Immun, DOI 10.1016/j.bbi.2018.09.005(2018).
[17] Y. Piontkewitz, M. Arad, I. Weiner, Tracing the development of psychosis and its prevention: what can be learned from animal models, Neuropharmacology, 62 (2012) 1273-1289.
[18] Y. Piontkewitz, M. Arad, I. Weiner, Risperidone administered during asymptomatic period of adolescence prevents the emergence of brain structural pathology and behavioral abnormalities in an animal model of schizophrenia, Schizophr Bull, 37 (2011) 1257-1269.
[19] Y. Piontkewitz, Y. Assaf, I. Weiner, Clozapine administration in adolescence prevents postpubertal emergence of brain structural pathology in an animal model of schizophrenia, Biol Psychiatry, 66 (2009) 1038-1046.
[20] A.C. Kentner, S.D. Bilbo, A.S. Brown, E.Y. Hsiao, A.K. McAllister, U. Meyer, B.D. Pearce, M.V. Pletnikov, R.H. Yolken, M.D. Bauman, Maternal immune activation: reporting guidelines to improve the rigor, reproducibility, and transparency of the model, Neuropsychopharmacology, DOI 10.1038/s41386-018-0185-7(2018).
[21] A.C. Vernon, S. Natesan, M. Modo, S. Kapur, Effect of chronic antipsychotic treatment on brain structure: a serial magnetic resonance imaging study with ex vivo and postmortem confirmation, Biol Psychiatry, 69 (2011) 936-944.

[22] T.C. Wood, C. Simmons, S.A. Hurley, A.C. Vernon, J. Torres, F. Dell'Acqua, S.C. Williams, D. Cash, Whole-brain ex-vivo quantitative MRI of the cuprizone mouse model, PeerJ, 4 (2016) e2632.
[23] E. Calabrese, A. Badea, C. Watson, G.A. Johnson, A quantitative magnetic resonance histology atlas of postnatal rat brain development with regional estimates of growth and variability, Neuroimage, 71 (2013) 196-206.
[24] C.R. Genovese, N.A. Lazar, T. Nichols, Thresholding of statistical maps in functional neuroimaging using the false discovery rate, Neuroimage, 15 (2002) 870-878.
[25] Q. Li, C. Cheung, R. Wei, V. Cheung, E.S. Hui, Y.Q. You, P. Wong, S.E. Chua, G.M. McAlonan, E.X. Wu, Voxel-based analysis of postnatal white matter microstructure in mice exposed to immune challenge in early or late pregnancy, Neuroimage, 52 (2010) 1-8.
[26] A. Bertero, A. Liska, M. Pagani, R. Parolisi, M.E. Masferrer, M. Gritti, M. Pedrazzoli, A. Galbusera, A. Sarica, A. Cerasa, M. Buffelli, R. Tonini, A. Buffo, C. Gross, M. Pasqualetti, A. Gozzi, Autism-associated 16p11.2 microdeletion impairs prefrontal functional connectivity in mouse and human, Brain, 141 (2018) 2055-2065.
[27] T.D. Satterthwaite, D.H. Wolf, M.E. Calkins, S.N. Vandekar, G. Erus, K. Ruparel, D.R. Roalf, K.A. Linn, M.A. Elliott, T.M. Moore, H. Hakonarson, R.T. Shinohara, C. Davatzikos, R.C. Gur, R.E. Gur, Structural Brain Abnormalities in Youth With Psychosis Spectrum Symptoms, JAMA Psychiatry, 73 (2016) 515-524.
[28] T.F. Nugent, 3rd, D.H. Herman, A. Ordonez, D. Greenstein, K.M. Hayashi, M. Lenane, L. Clasen, D. Jung, A.W. Toga, J.N. Giedd, J.L. Rapoport, P.M. Thompson, N. Gogtay, Dynamic mapping of hippocampal development in childhood onset schizophrenia, Schizophr Res, 90 (2007) 62-70.
[29] R.M. Yoder, K.C. Pang, Involvement of GABAergic and cholinergic medial septal neurons in hippocampal theta rhythm, Hippocampus, 15 (2005) 381-392.
[30] C.Y. Huh, R. Goutagny, S. Williams, Glutamatergic neurons of the mouse medial septum and diagonal band of Broca synaptically drive hippocampal pyramidal cells: relevance for hippocampal theta rhythm, J Neurosci, 30 (2010) 15951-15961.
[31] E. Gould, N.J. Woolf, L.L. Butcher, Postnatal development of cholinergic neurons in the rat: I. Forebrain, Brain Res Bull, 27 (1991) 767-789.
[32] L. Pratt, L. Ni, N.M. Ponzio, G.M. Jonakait, Maternal inflammation promotes fetal microglial activation and increased cholinergic expression in the fetal basal forebrain: role of interleukin-6, Pediatr Res, 74 (2013) 393-401.
[33] T.L. Kemper, M. Bauman, Neuropathology of infantile autism, J Neuropathol Exp Neurol, 57 (1998) 645-652.
[34] R. Brisch, H.G. Bernstein, H. Dobrowolny, M. Krzyzanowska, Z. Jankowski, B. Bogerts, T. Gos, Volumetric analysis of the diagonal band of Broca in patients with schizophrenia and affective disorders: A post-mortem study, Clin Anat, 29 (2016) 466-472.
[35] T. Notter, J.M. Coughlin, A. Sawa, U. Meyer, Reconceptualization of translocator protein as a biomarker of neuroinflammation in psychiatry, Mol Psychiatry, 23 (2018) 36-47.
[36] S. Smolders, T. Notter, S.M.T. Smolders, J.M. Rigo, B. Brone, Controversies and prospects about microglia in maternal immune activation models for neurodevelopmental disorders, Brain Behav Immun, 73 (2018) 51-65.

[37] J.J. Roland, A.L. Stewart, K.L. Janke, M.R. Gielow, J.A. Kostek, L.M. Savage, R.J. Servatius, K.C. Pang, Medial septum-diagonal band of Broca (MSDB) GABAergic regulation of hippocampal acetylcholine efflux is dependent on cognitive demands, J Neurosci, 34 (2014) 506-514.
[38] D.D. Dickerson, A.R. Wolff, D.K. Bilkey, Abnormal long-range neural synchrony in a maternal immune activation animal model of schizophrenia, J Neurosci, 30 (2010) 12424-12431.
[39] G. Ducharme, G.C. Lowe, R. Goutagny, S. Williams, Early alterations in hippocampal circuitry and theta rhythm generation in a mouse model of prenatal infection: implications for schizophrenia, PLoS One, 7 (2012) e29754.
[40] M.C. van Eede, J. Scholz, M.M. Chakravarty, R.M. Henkelman, J.P. Lerch, Mapping registration sensitivity in MR mouse brain images, Neuroimage, 82 (2013) 226-236.
[41] E. Thomas, A. Graham, M. Rudolph, J. Rasmussen, P. Wadhwa, S. Entringer, J. Gilmore, M. Styner, C. Buss, D. Fair, Implications of Newborn Amygdala Connectivity on Fear Vs. Negative Emotionality Development over the First Year of Life, Biol Psychiat, 81 (2017) S100-S100.

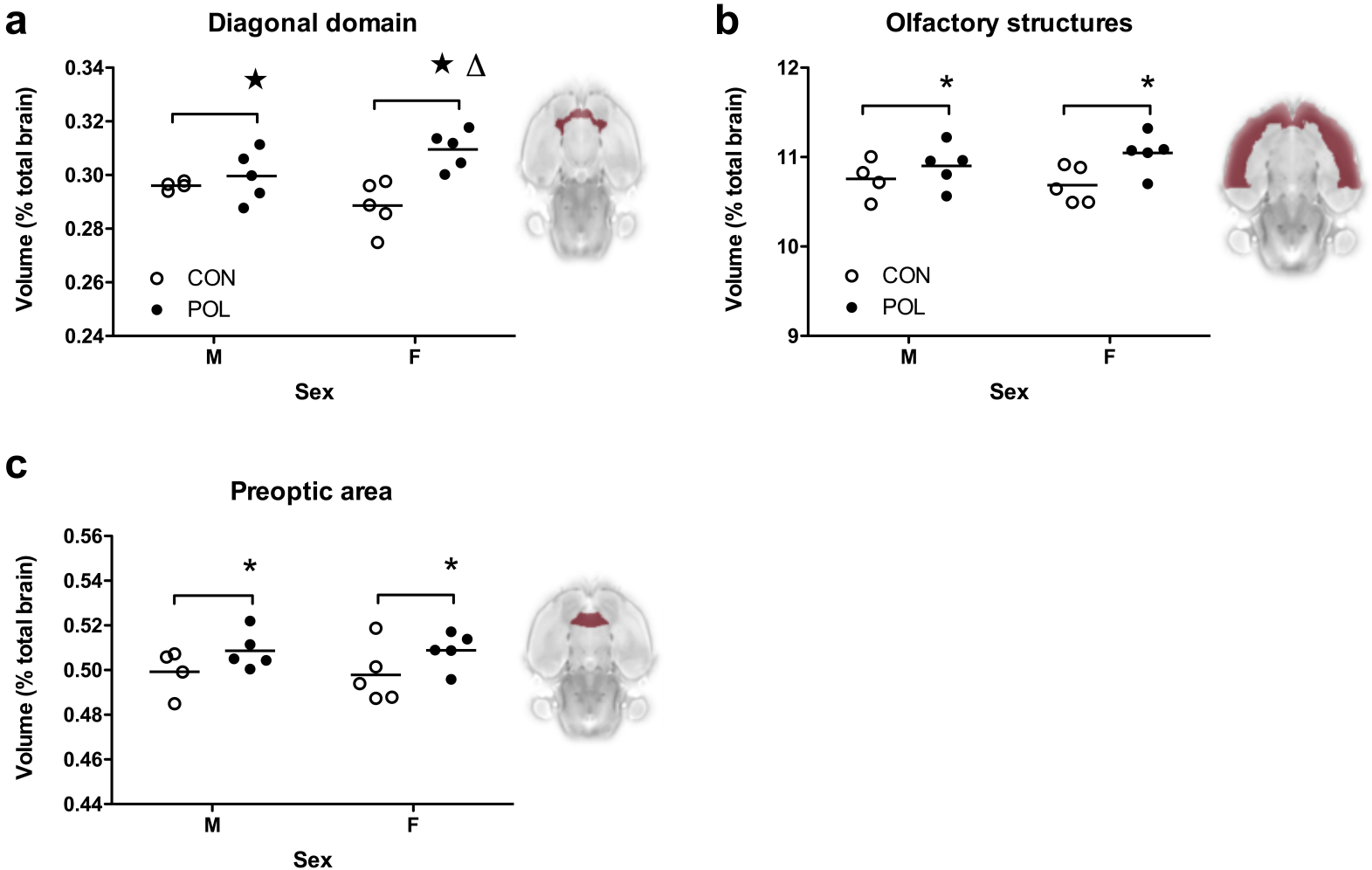
a
Diagonal domain
Volume (% total brain)
0.34
0.32
0.30
0.28
0.26
0.24
★
★ Δ
CON
POL
M
F
Sex
b
Olfactory structures
Volume (% total brain)
12
11
10
9
*
*
CON
POL
M
F
Sex
c
Preoptic area
Volume (% total brain)
0.56
0.54
0.52
0.50
0.48
0.46
0.44
*
*
M
F
Sex

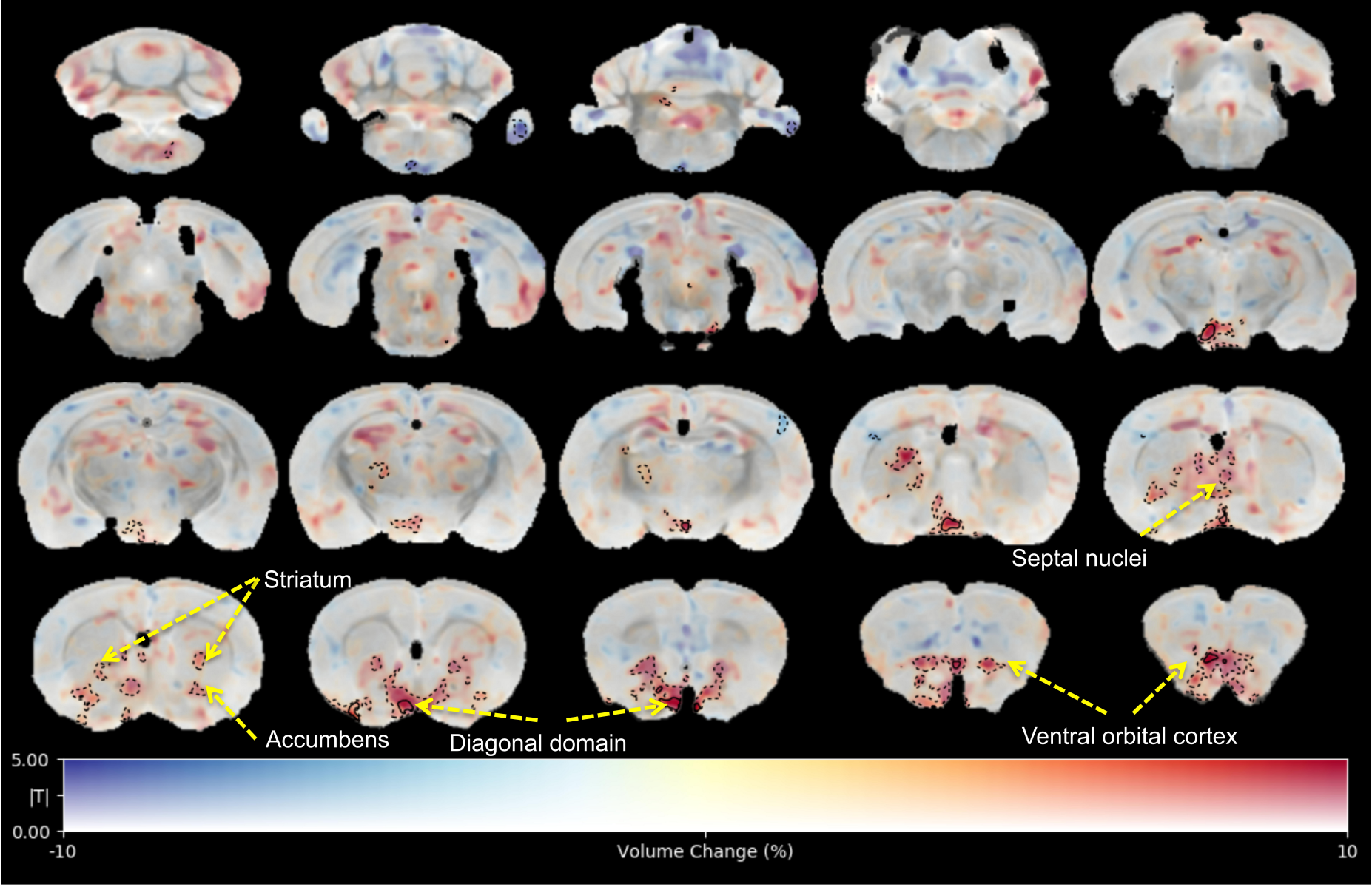

Significance level indicated by contours: p<0.05 (uncorrected) p<0.005 (uncorrected)

Region of interest	**Two way ANOVA**			***Post-hoc* test***
	Within subjects		**Between groups**	
	Sex (*p*, *q*)	**MIA x Sex interaction (*p*, *q*)**	**MIA (*p*, *q*)**	
Whole brain	*F(1,15)=5.89; p<0.05 (q>0.1)*	F(1,15)=3.32; p>0.05 (q>0.1)	F(1,15)=0.31; p>0.05 (q>0.1)	None
BNST	*F(1,15)=4.97; p<0.05 (q>0.1)*	F(1,15)=0.16; p>0.05 (q>0.1)	F(1,15)=0.01; p>0.05 (q>0.1)	None
Cerebellum	*F(1,15)=4.40; p<0.05 (q>0.1)*	F(1,15)=1.25; p>0.05 (q>0.1)	F(1,15)=0.44; p>0.05 (q>0.1)	None
Lateral ventricles	F(1,15)=4.34; p<0.05 (q>0.1)	F(1,15)=0.09; p>0.05 (q>0.1)	F(1,15)=0.01; p>0.05 (q>0.1)	None
Diagonal domain	F(1,15)=0.12; p>0.05 (q>0.1)	**F(1,15)=11.8; p<0.01 (q<0.1)**	*F(1,15)=5.91; p<0.05 (q>0.1)*	PF > CF
Olfactory structures	F(1,15)=0.13; p>0.05 (q>0.1)	*F(1,15)=6.11; p<0.05 (q>0.1)*	F(1,15)=1.07; p>0.05 (q>0.1)	None
Preoptic area	F(1,15)=0.02; p>0.05 (q>0.1)	*F(1,15)=4.77; p<0.05 (q>0.1)*	F(1,15)=0.03; p>0.05 (q>0.1)	None
Nucleus accumbens	F(1,15)=1.06; p>0.05 (q>0.1)	F(1,15)=2.19; p>0.05 (q>0.1)	*F(1,15)=5.49; p<0.05 (q>0.1)*	PF > CF
Pineal gland	F(1,15)=1.21; p>0.05 (q>0.1)	F(1,15)=1.86; p>0.05 (q>0.1)	*F(1,15)=9.18; p<0.01 (q>0.1)*	PM < CM
Anterior commissure	F(1,15)=0.41; p>0.05 (q>0.1)	F(1,15)=0.10; p>0.05 (q>0.1)	*F(1,15)=5.11; p<0.05 (q>0.1)*	PM < CM